Title

Comparison of diffusion-weighted imaging and T2-weighted single shot fast spin-echo: Implications for LI-RADS characterization of hepatocellular carcinoma

Journal

Magnetic Resonance Imaging, 34(7)

ISSN

0730-725X

Authors

Hicks, Robert M
Yee, Judy
Ohliger, Michael A
et al.

Publication Date

2016-09-01

DOI

10.1016/j.mri.2016.04.007

Peer reviewed

HHS Public Access

Author manuscript

Magn Reson Imaging. Author manuscript; available in PMC 2017 March 01.

Published in final edited form as:

Magn Reson Imaging. 2016 September ; 34(7): 915–921. doi:10.1016/j.mri.2016.04.007.

Comparison of diffusion-weighted imaging and T2-weighted single shot fast spin-echo: Implications for LI-RADS characterization of hepatocellular carcinoma

Robert M. Hicks[a], **Judy Yee**[a,b], **Michael A. Ohliger**[a,c], **Stefanie Weinstein**[a,b], **Jeffrey Kao**[a,b], **Nabia S. Ikram**[a,b], and **Thomas A. Hope**[a,b,*]

[a]Department of Radiology and Biomedical Imaging, University of California, San Francisco, San Francisco, CA, USA

[b]Department of Radiology, Veterans Affairs Medical Center, University of California, San Francisco, San Francisco, CA, USA

[c]Department of Radiology, Zuckerberg San Francisco General Hospital, San Francisco, CA, USA

Abstract

Purpose—To evaluate the performance of diffusion-weighted imaging (DWI) and T2-weighted single shot fast spin-echo (SSFSE) imaging of the liver in the detection of hepatocellular carcinoma (HCC) in reference to the LI-RADS classification system.

Methods—MR images of 40 patients with 68 LI-RADS grade 3–5 lesions were analyzed. Two readers independently reviewed sequences and characterized lesion signal intensity, followed by consensus evaluation. CE-MRI served as reference standard. Sensitivities were compared across sequences. Lesion-to-liver contrast-to-noise ratios (CNRs) and apparent diffusion coefficients (ADCs) were measured and compared using the Wilcoxon signed-rank test across sequences and the Mann–Whitney U or Kruskal–Wallis test between LI-RADS categories. Inter-reader variability was assessed using Cohen's kappa statistic.

Results—Consensus sensitivities of LI-RADS 3–5 lesions using SSFSE images versus DWI were similar (0.53–0.63, $p = 0.089$), however, the sensitivity with DWI b = 700 was higher (0.63) than DWI b = 0 (0.53, $p = 0.039$). Lesion-to-liver CNRs were larger for all DWI sequences compared to SSFSE images ($p < 0.001$ for all). ADCs of large (>2 cm) LIRADS 3–5 lesions were lower than those of small lesions (1.09 ± 0.33 vs. 1.31 ± 0.26, $p = 0.02$), however lesion ADCs were not different from those of adjacent hepatic parenchyma for any LI-RADS lesion.

Conclusions—DWI has a similar sensitivity compared to SSFSE, but intensity on DWI likely represents intrinsic T2 signal hyper-intensity rather than restricted diffusion as the ADC values were not lower than adjacent parenchyma. Therefore it may not be appropriate to consider hyper-intensity on high b-value as a separate ancillary criteria to T2 hyper-intensity in LI-RADS.

*Corresponding author at: Department of Radiology and Biomedical Imaging, School of Medicine, University of California, 505 Parnassus Avenue, San Francisco, CA, 94143-0628, USA. Tel.: +1 415 476 1537; fax: +1 415 476 0616. Thomas.hope@ucsf.edu (T.A. Hope).

Keywords

Hepatocellular carcinoma; Diffusion-weighted imaging; MRI; LI-RADS

1. Introduction

Hepatocellular carcinom a (HCC) is the most common primary liver malignancy and the second most common cause of cancer death worldwide [1]. The Liver Imaging Reporting and Data System (LI-RADS) was introduced by the ACR in 2011 (updated 2013 and 2014) and is designed to standardize radiologic diagnosis of HCC [2,3]. Five major criteria are used to assign LI-RADS category: size, arterial phase hyper-enhancement, washout appearance, capsule appearance, and threshold growth. There are multiple ancillary features that can be used to upgrade LI-RADS category, including mild T2 hyper-intensity and hyper-intensity on diffusion-weighted images (DWI).

T2-weighted imaging techniques are sensitive for the detection of focal liver lesions (FLLs), and serve as an adjunct to contrast-enhanced magnetic resonance imaging (CE-MRI) for LI-RADS classification [4]. These sequences are routinely performed using either single shot fast spin-echo (SSFSE) techniques or fast spin-echo (FSE) techniques. A breath-hold half-Fourier single-shot fast spin echo is used for T2-weighted images in order to minimize respiratory artifact that corrupts fast spin echo T2-weighted techniques, while maintaining high lesion contrast relative to the liver [5,6]. While FSE approaches may have less T2 blurring and improved contrast, the overall sensitivity for FLLs is similar [7].

DWI has been shown to be effective for detection and characterization of HCC in cirrhotic patients [8,9]. DWI sequences are conventionally obtained with multiple diffusion sensitivities (b-values). DWI without diffusion sensitizing gradients (b = 0), has predominantly T2 contrast with a shorter read-out time than single shot or fast spin echo techniques. These b = 0 images can be difficult to interpret due to the significant signal in adjacent vessels. Therefore groups have used low b-value images (b = 25–100) to minimize signal from adjacent vasculature by attenuating bulk flow in capillaries and small vessels, and have shown increased sensitivity in detection of focal liver lesions [10,11]. For lesions that have true restricted diffusion, high b-value images should have a higher sensitivity for detection compared to low b-value images. This has been well demonstrated for non-hepatocellular lesions such as metastasis [12–14]. However, this association is less clear with HCC, as there is considerable overlap between the apparent diffusion coefficient (ADC) in HCC lesions and adjacent hepatic parenchyma [15–18].

Several studies have compared the sensitivity of T2-weighted imaging to DWI for the detection of focal liver lesions [11,19–21]. These studies have shown increased sensitivity of low b-value DWI for HCC detection when compared to conventional T2-weighted sequences, especially in the case of smaller lesions [22]. However, there is no consensus on the optimal b-value for detection of HCC in cirrhosis [23]. Moreover, there are no studies that compare HCC detection using DWI with multiple b-values to T2-weighted imaging, with consensus CE-MRI and the LI-RADS classification system as the standard of reference. The purpose of this study was to evaluate HCC lesion conspicuity using both low

(b = 0, 50) and high b-value (b = 700) DWI and T2-weighted image series, in relation to the LI-RADS classification system.

2. Materials and methods

2.1. Patients

Between January 2014 and June 2014, 90 consecutive patients suspected of having HCC or secondary liver malignancies underwent MR imaging at our institution, a Veteran's Administration hospital. Forty-five patients had suspicious liver lesions and eligible for inclusion. Five patients with proven metastases (n = 1 cholangio-carcinoma, n = 2 peripheral neuroendocrine tumors, n = 1 rectal adenocarcinoma and n = 1 colon adenocarcinoma) were excluded. Thus, forty patients were included in the analysis. All patients were male with a median age of 63 years (IQR 60–67). Thirty-two patients had been previously treated for HCC, either with transcatheter arterial chemoembolization, radiofrequency ablation or tumor resection. In these patients only untreated lesions separate from previous treatment sites were considered for analysis. Eight patients with HCC were treatment-naïve, all of whom had cirrhosis due to hepatitis C virus.

2.2. MR imaging techniques

All imaging studies were performed on a 3.0 TMR system (Skyra, Siemens, Erlangen, Germany). An 18 channel anterior array was used in combination with a 12 channel posterior array. Transverse T2-weighted single shot turbo spin echo (HASTE) images were acquired with the following acquisition parameters: effective echo time, 95 ms; flip angle, 160; matrix size, 320 × 219; field of view, 470 × 400 mm; signal averages, 1; parallel imaging factor of 2 with 42 center lines for a total of 219 echos; fat saturation was achieved using spectrally adiabatic inversion recovery (SPAIR); slice thickness, 5 mm with a 1 mm gap; and 37 slices total using 4 concatenations resulting in four 16 s breath-holds.

DWI was acquired with the following parameters: TR/TE, 1800/55 ms; bandwidth, 2604 Hz; matrix size, 128 × 112; field of view, 360 × 315 mm; slice thickness 6 mm with 1.2 mm gaps; GRAPPA parallel imaging acceleration factor of 2 utilizing 24 center lines for a total of 112 echoes. Three b-values were used, b = 0/50/700 s/mm^3, with 2, 2 and 6 signal averages for each b-value respectively. A higher number of averages was used for b = 700 images due to the lower signal-to-noise, and two averages was used for the lower b-values to attempt to minimize image misregistration due to motion artifact. Diffusion sensitizing gradients were selected so that all three gradients were played simultaneously in order to minimize the echo time; by doing so the echo time was reduced from 67 ms to 55 ms. Respiratory navigators were used. The majority of acquisitions took less than two minutes to acquire depending on respiratory trigger acceptance.

2.3. Standard of reference and consensus evaluation

Lesions identified by consensus using dynamic CE-MRI using Gadavist (Bayer Healthcare, Wayne, NJ) served as the standard of reference and for LI-RADS v2014 classification. Each study was reviewed for the presence of LI-RADS 3–5 lesions. Lesion size, liver segment, and LI-RADS classification were recorded. Of note, T2 signal intensity and DWI

characteristics were not included for LI-RADS classification. Hepatobiliary phase imaging was also performed using gadoxetate disodium (Eovist, Bayer Healthcare), and lesions that were seen only as hypo-intense on the hepatobiliary phase were graded as LI-RADS 3 if <2 cm and LI-RADS 4 if ≥2 cm. Only lesions ≥1.0 cm in largest diameter were included for analysis, and up to four liver lesions per patient were included for analysis to limit clustering bias. Nodular lesions adjacent to but separate from previous treatment sites were classified according to LI-RADS criteria.

2.4. Qualitative analysis

Analysis of all MR images was performed on a PACS workstation (Intellispace, Philips Healthcare). Two abdominal radiologists (with three and ten years experience) retrospectively and independently reviewed all images and served as the consensus. The observers were blinded to MR imaging reports and clinical history. Observers were provided a spreadsheet containing the corresponding CE-MRI image number and liver segment for each lesion. For lesion detection with DWI, the observers analyzed images with b values of 0, 50, and 700 in series. The observers were instructed to score lesions as either hyper-, iso-, or hypo-intense relative to the surrounding liver parenchyma. The same scoring system was used for T2-weighted images. A consensus read was performed when there was disagreement between the two readers.

Each observer independently evaluated the degree of image quality degradation caused by respiratory ghost, pulsatile blood flow ghost, and susceptibility artifacts using a four-point scale (1 = absent or minimal, 2 = mild, 3 = moderate, 4 = severe). A “severe” score indicated that an image was uninterpretable and a “mild” score indicated that the artifact did not affect interpretation. Scores of 1 and 2 indicated images of overall excellent and good quality, respectively.

2.5. Quantitative lesion analysis

Quantitative analysis was conducted using region of interest (ROI) measurements for all lesions identified on T2-weighted images and/or DWI, using OsiriX [24]. Liver lesion signal intensity was measured with ROIs drawn to encompass as much of the lesion as possible, while leaving 1–2 mm of lesion surrounding the margins. ROI size was identical between T2 and DWI sequence. Signal intensity in the adjacent hepatic parenchyma was calculated from the average of two ROIs, each identical in size to the liver lesion ROI, placed in areas devoid of large vessels, focal signal intensity changes, and artifacts. Lesion-to-liver contrast-to-noise ratios (CNR) were calculated with the equation $(SI_{lesion} - SI_{liver})/SD$, where SI_{lesion} and SI_{liver} are the respective signal intensities of the liver and lesion and SD is the standard deviation of the signal intensities in the adjacent liver [19,21,4]. The quantitative analysis was only performed on lesions that were identified as hyper-intense on either the T2-weighted or on at least one DWI sequence.

ADC measurements were calculated using the two b-values estimator (ADC_2) [25,26]:

$$\frac{\ln\ s_1 - \ln\ s_2}{b_2 - b_1} = ADC$$

where b_1, b_2, are the b-values used to acquire the signal s_1, s_2, and ADC is the unknown parameter. Signals b_1 and b_2 corresponded to b = 0 and b = 700. ADC values (mm^2/s) of lesions and liver parenchyma were calculated from the same ROIs placed for signal intensity measurements, in order to limit artifact from misregistration on calculated ADC maps.

2.6. Statistical analysis

For the qualitative analysis, sensitivity was computed as the percentage of suspicious lesions that were visibly hyper-intense for each type of sequence when compared to the reference standard CE-MRI. For each reader, the Friedman's test was used for overall comparison of sensitivity among all four sequences, and the Wilcoxon signed-rank test was used for each pairwise comparison. Cohen's Kappa statistic was used to assess inter-reader agreement for lesion detection (0–0.2 indicated slight agreement; 0.21–0.4, fair agreement; 0.41–0.6, moderate agreement; 0.61–0.8, substantial agreement and 0.81–1.00, almost perfect agreement) [27]. For the quantitative analysis, the Kruskal–Wallis or Mann–Whitney U test were used when comparing lesion-to-liver CNR and ADC maps across LI-RADS classification and lesion size, respectively. All p-values were two sided with $p < 0.05$ considered statistically significant.

3. Results

3.1. Lesion detection, inter-reader agreement and image quality

Sixty-eight lesions in 40 patients were reviewed. In total, 19, 38, and 11 LI-RADS 5, 4, and 3 lesions were included for analysis, respectively.

The overall sensitivity of the T2-weighted image sequence was 0.63 (51/81 lesions) for reader 1 and 0.69 (56/81 lesions) for reader 2. Table 1). The overall sensitivities of the DWI images ranged from 0.56 (45/81, b = 0) to 0.68 (55/81, b = 700) for reader 1, and from 0.57 (46/81, b = 0) to 0.75 (61/81, b = 700) for reader 2. For pairwise comparisons of sequence sensitivities, the consensus panel detected more lesions with the DWI b = 700 than with b = 0 sequence (p = 0.039). Analysis of LI-RADS 3–5 lesions alone (n = 68) also showed a higher sensitivity with b = 700 compared to b = 0 (p = 0.039) (Figure 2 and 3).

Inter-reader agreement for sensitivity ranged from substantial ($\kappa = 0.65$ for DWI b = 0) to almost perfect ($\kappa = 0.79$ for T2-weighted sequence) across all pair-wise comparisons of sequences.

Overall image degradation due to artifact in DWI was rated as absent or minimal in all 40 cases. Mild respiratory artifact was noted in 18 DWI and 13 T2-weighted image sequences, respectively, but no sequence had moderate to severe artifacts.

3.2. Contrast-to-noise and ADC maps

Quantitative analysis of the 49 lesions detected in the T2-weighted and/or DWI sequences revealed significantly higher CNR among all DWI sequences compared to the T2-weighted image sequence (Figure 1 and 4, Table 2). There was no significant difference in CNR between different b-values. Comparison of CNR across LI-RADS categories showed a trend

of increased CNR with higher LI-RADS classification in all DWI sequences, reaching statistical significance with b = 0 (p = 0.027).

ADCs were not significantly different from the ADCs of surrounding liver parenchyma (p = 0.67 and 0.69, respectively) (Table 3). However, when lesions were stratified by size (<2 cm or ≥2 cm), larger lesions had lower ADC values compared to smaller lesions (p = 0.02). Smaller lesions had higher ADC values than the surrounding liver parenchyma (p = 0.045).

Of the lesions that were not detected on any one of the four sequences, 7 were LI-RADS 3 lesions, 12 were LI-RADS 4 lesions, and 1 was a LI-RADS 5 lesion.

4. Discussion

Determination of the presence of mild T2 hyper-intensity or restricted diffusion is important in the diagnosis of HCC as both are ancillary features in the LI-RADS algorithm. In our study we show that DWI has increased quantitative lesion conspicuity than T2-weighted imaging. Clinically, this finding is important because radiologic T-stage is based on the number and size of observed LI-RADS 5 lesions, and lesion detection due to high CNR may lead to characterization with other sequences. However, the two sequences did not differ in terms of qualitative rates of lesion detection. Additionally, neither small nor large HCCs had lower ADC values than adjacent parenchyma.

Prior literature has focused on ADC cutoffs between benign (cyst and hemangioma) and malignant (HCC and metastasis) lesions, but in clinical evaluation, this difference would be determined typically with other imaging findings such as enhancement characteristics [14–18]. In this way, “restricted” diffusion has been proposed as a way of discriminating between cysts and malignant lesions, as an ADC similar to adjacent hepatic parenchyma excludes cyst from the diagnosis [14]. In the LI-RADS algorithm, restricted diffusion is defined as lesion hyper-intensity on high b-value weighted sequences with an ADC value similar to or lower than adjacent parenchyma. In this setting, diffusion weighted imaging is being used to suggest a malignant potential of a solid lesion rather than differentiate it from a cyst. We demonstrate that although LI-RADS 3–5 lesions frequently demonstrate hyper-intense signal on high b-value images, absence of corresponding decrease in ADC values compared to adjacent parenchyma suggests that this hyper-intense signal is related to intrinsic T2 hyper-intensity rather than to true diffusion restriction relative to adjacent parenchyma [28]. Therefore if one defines restricted diffusion as hyper-intensity on high b-value image, it would be prudent to combine T2 hyper-intensity and restricted diffusion into a single ancillary feature as they likely are imaging identical characteristics.

When creating a liver protocol, our results may inform sequence selection. If DWI and T2-weighted sequences are imaging the same endpoints, it may be possible to omit one sequence from the imaging protocol. High b-value images are significantly more time intensive to acquire than low b-value images due to the decreased signal-to--noise in the acquired data. In the technique that we used, we averaged the b = 700 image 6 times whereas we only used two averages for the B = 50 image. Therefore if we were to remove

the B = 700 images we could reduce the time of acquisition for our diffusion weighted images by 80%.

Likely the physiologic information on DWI sequences is not centered on the changes in diffusion, but rather the intrinsic T2 signal intensity of the lesion. One thing to consider when comparing single shot T2 techniques to DWI is that the echo planar readout in DWI is much shorter. The readout of a single shot fast spin echo may take 400 to 500 ms while in DWI the readout lasts 20 to 30 ms. This decreased readout time will decrease T2 blurring and may increase contrast for lesions with intermediate T2 signal. We were not able to demonstrate this theoretical advantage of DWI over the single shot technique in our data.

There are many limitations in this study. First we had a small number of lesions, which may lead to a failure to detect a significant difference in sensitivity between T2-weighted imaging and DWI. Additionally we only considered untreated lesions. It has been demonstrated previously that after focal therapy, disease recurrence on DWI does correlate with reduced ADCs compared to adjacent hepatic parenchyma [29]. Therefore our results should not be extrapolated to the post-treatment population. It should also be noted that ADC measurements are variable between sites and our results should not be used to create ADC cutoffs for disease at other sites [30].

An additional bias in our study is that all of our patients had cirrhosis, predominantly secondary to HCV. As the ADC of cirrhotic liver is lower than in the non-cirrhotic population, the HCCs imaged may have demonstrated lower ADCs than adjacent hepatic parenchyma if they had occurred in non-cirrhotic patients [31,32]. Therefore in the setting of non-cirrhotic HBV patients, decreased ADC values may be visualized.

In conclusion, we have shown that DWI has a similar sensitivity for the detection of hepatic lesions compared to single shot fast spin echo, but that the signal intensity seen on DWI probably represents intrinsic T2 signal hyper-intensity rather than restricted diffusion as the ADC values were not lower than the adjacent hepatic parenchyma. Therefore hyper-intensity on high b-value images should not be considered a separate ancillary criterion to hyper--intensity on T2-weighted images in the LI-RADS algorithm.

Acknowledgments

MO is supported in part by a Pilot/Feasibility Grant from the UCSF Liver Center (P30 DK026743)

References

1. Stewart, BW., Wild, CP. World cancer report 2014. IARC; 2014.
2. Radiology ACo. Liver imaging reporting and data system version 2013.1. American College of Radiology. 2013 [Accessed 08/10/2014 2014] http://www.acr.org/Quality-Safety/Resources/LIRADS/.
3. Cruite I, Tang A, Sirlin CB. Imaging-based diagnostic systems for hepatocellular carcinoma. AJR Am J Roentgenol. 2013; 201(1):41–55. http://dx.doi.org/10.2214/AJR.13.10570. [PubMed: 23789657]
4. Matsuo M, Kanematsu M, Murakami T, Kim T, Hori M, Kondo H, et al. T2-weighted MR imaging for focal hepatic lesion detection: supplementary value of breath-hold imaging with half-Fourier

single-shot fast spin-echo and multishot spin-echo echoplanar sequences. J Magn Reson Imaging. 2000; 12(3):444–452. [PubMed: 10992312]

5. Tang Y, Yamashita Y, Namimoto T, Abe Y, Takahashi M. Liver T2-weighted MR imaging: comparison of fast and conventional half-Fourier single-shot turbo spin-echo, breath-hold turbo spin-echo, and respiratory-triggered turbo spin-echo sequences. Radiology. 1997; 203(3):766–772. http://dx.doi.org/10.1148/radiology.203.3.9169702. [PubMed: 9169702]
6. Gaa J, Hatabu H, Jenkins RL, Finn JP, Edelman RR. Liver masses: replacement of conventional T2-weighted spin-echo MR imaging with breath-hold MR imaging. Radiology. 1996; 200(2):459–464. http://dx.doi.org/10.1148/radiology.200.2.8685342. [PubMed: 8685342]
7. Hori M, Murakami T, Kim T, Kanematsu M, Tsuda K, Takahashi S, et al. Single breath-hold T2-weighted MR imaging of the liver: value of single-shot fast spin-echo and multishot spin-echo echoplanar imaging. AJR Am J Roentgenol. 2000; 174(5):1423–1431. http://dx.doi.org/10.2214/ajr.174.5.1741423. [PubMed: 10789807]
8. Piana G, Trinquart L, Meskine N, Barrau V, Beers BV, Vilgrain V. New MR imaging criteria with a diffusion-weighted sequence for the diagnosis of hepatocellular carcinoma in chronic liver diseases. J Hepatol. 2011; 55(1):126–132. http://dx.doi.org/10.1016/j.jhep.2010.10.023. [PubMed: 21145857]
9. Xu PJ, Yan FH, Wang JH, Shan Y, Ji Y, Chen CZ. Contribution of diffusion-weighted magnetic resonance imaging in the characterization of hepatocellular carcinomas and dysplastic nodules in cirrhotic liver. J Comput Assist Tomogr. 2010; 34(4):506–512. http://dx.doi.org/10.1097/RCT.0b013e3181da3671. [PubMed: 20657216]
10. Moteki T, Horikoshi H, Oya N, Aoki J, Endo K. Evaluation of hepatic lesions and hepatic parenchyma using diffusion-weighted reordered turboFLASH magnetic resonance images. J Magn Reson Imaging. 2002; 15(5):564–572. http://dx.doi.org/10.1002/jmri.10101. [PubMed: 11997898]
11. Zech CJ, Herrmann KA, Dietrich O, Horger W, Reiser MF, Schoenberg SO. Black-blood diffusion-weighted EPI acquisition of the liver with parallel imaging: comparison with a standard T2-weighted sequence for detection of focal liver lesions. Investig Radiol. 2008; 43(4):261–266. http://dx.doi.org/10.1097/RLI.0b013e31816200b5. [PubMed: 18340250]
12. Gourtsoyianni S, Papanikolaou N, Yarmenitis S, Maris T, Karantanas A, Gourtsoyiannis N. Respiratory gated diffusion-weighted imaging of the liver: value of apparent diffusion coefficient measurements in the differentiation between most commonly encountered benign and malignant focal liver lesions. Eur Radiol. 2008; 18(3):486–492. http://dx.doi.org/10.1007/s00330-007-0798-4. [PubMed: 17994317]
13. Onur MR, Cicekci M, Kayali A, Poyraz AK, Kocakoc E. The role of ADC measurement in differential diagnosis of focal hepatic lesions. Eur J Radiol. 2012; 81(3):e171–e176. http://dx.doi.org/10.1016/j.ejrad.2011.01.116. [PubMed: 21353418]
14. Taouli B, Vilgrain V, Dumont E, Daire JL, Fan B, Menu Y. Evaluation of liver diffusion isotropy and characterization of focal hepatic lesions with two single-shot echo-planar MR imaging sequences: prospective study in 66 patients. Radiology. 2003; 226(1):71–78. http://dx.doi.org/10.1148/radiol.2261011904. [PubMed: 12511671]
15. Ichikawa T, Erturk SM, Motosugi U, Sou H, Iino H, Araki T, et al. High-B-value diffusion-weighted MRI in colorectal cancer. AJR Am J Roentgenol. 2006; 187(1):181–184. http://dx.doi.org/10.2214/AJR.05.1005. [PubMed: 16794174]
16. Tamai K, Koyama T, Saga T, Umeoka S, Mikami Y, Fujii S, et al. Diffusion-weighted MR imaging of uterine endometrial cancer. J Magn Reson Imaging. 2007; 26(3):682–687. http://dx.doi.org/10.1002/jmri.20997. [PubMed: 17729360]
17. Bruegel M, Holzapfel K, Gaa J, Woertler K, Waldt S, Kiefer B, et al. Characterization of focal liver lesions by ADC measurements using a respiratory triggered diffusion-weighted single-shot echo-planar MR imaging technique. Eur Radiol. 2008; 18(3):477–485. http://dx.doi.org/10.1007/s00330-007-0785-9. [PubMed: 17960390]
18. Miller FH, Hammond N, Siddiqi AJ, Shroff S, Khatri G, Wang Y, et al. Utility of diffusion-weighted MRI in distinguishing benign and malignant hepatic lesions. J Magn Reson Imaging. 2010; 32(1):138–147. http://dx.doi.org/10.1002/jmri.22235. [PubMed: 20578020]
19. Hussain SM, De Becker J, Hop WC, Dwarkasing S, Wielopolski PA. Can a single-shot black-blood T2-weighted spin-echo echo-planar imaging sequence with sensitivity encoding replace the respiratory-triggered turbo spin-echo sequence for the liver? An optimization and feasibility study.

J Magn Reson Imaging. 2005; 21(3):219–229. http://dx.doi.org/10.1002/jmri.20269. [PubMed: 15723376]

20. Parikh T, Drew SJ, Lee VS, Wong S, Hecht EM, Babb JS, et al. Focal liver lesion detection and characterization with diffusion-weighted MR imaging: comparison with standard breath-hold T2-weighted imaging. Radiology. 2008; 246(3):812–822. http://dx.doi.org/10.1148/radiol.2463070432. [PubMed: 18223123]
21. Coenegrachts K, Delanote J, Ter Beek L, Haspeslagh M, Bipat S, Stoker J, et al. Improved focal liver lesion detection: comparison of single-shot diffusion-weighted echoplanar and single-shot T2 weighted turbo spin echo techniques. Br J Radiol. 2007; 80(955):524–531. http://dx.doi.org/10.1259/bjr/33156643. [PubMed: 17510250]
22. Okada Y, Ohtomo K, Kiryu S, Sasaki Y. Breath-hold T2-weighted MRI of hepatic tumors: value of echo planar imaging with diffusion-sensitizing gradient. J Comput Assist Tomogr. 1998; 22(3):364–371. [PubMed: 9606375]
23. Lim KS. Diffusion-weighted MRI of hepatocellular carcinoma in cirrhosis. Clin Radiol. 2014; 69(1):1–10. http://dx.doi.org/10.1016/j.crad.2013.07.022. [PubMed: 24034549]
24. Rosset A, Spadola L, Ratib O. OsiriX: an open-source software for navigating in multidimensional DICOM images. J Digit Imaging. 2004; 17(3):205–216. http://dx.doi.org/10.1007/s10278-004-1014-6. [PubMed: 15534753]
25. Freiman M, Voss SD, Mulkern RV, Perez-Rossello JM, Callahan MJ, Warfield SK. In vivo assessment of optimal b-value range for perfusion-insensitive apparent diffusion coefficient imaging. Med Phys. 2012; 39(8):4832–4839. http://dx.doi.org/10.1118/1.4736516. [PubMed: 22894409]
26. Stejskal EO, Tanner JE. Spin diffusion measurements: spin echoes in the presence of a time-dependent field gradient. J Chem Phys. 1965; 42(1):288–292. http://dx.doi.org/10.1063/1.1695690.
27. Landis JR, Koch GG. An application of hierarchical kappa-type statistics in the assessment of majority agreement among multiple observers. Biometrics. 1977; 33(2):363–374. [PubMed: 884196]
28. Taouli B, Koh DM. Diffusion-weighted MR imaging of the liver. Radiology. 2010; 254(1):47–66. http://dx.doi.org/10.1148/radiol.09090021. [PubMed: 20032142]
29. Schraml C, Schwenzer NF, Clasen S, Rempp HJ, Martirosian P, Claussen CD, et al. Navigator respiratory-triggered diffusion-weighted imaging in the follow-up after hepatic radiofrequency ablation-initial results. J Magn Reson Imaging. 2009; 29(6):1308–1316. http://dx.doi.org/10.1002/jmri.21770. [PubMed: 19418557]
30. Malyarenko D, Galban CJ, Londy FJ, Meyer CR, Johnson TD, Rehemtulla A, et al. Multi-system repeatability and reproducibility of apparent diffusion coefficient measurement using an ice-water phantom. J Magn Reson Imaging. 2013; 37(5):1238–1246. http://dx.doi.org/10.1002/jmri.23825. [PubMed: 23023785]
31. Muller MF, Prasad P, Siewert B, Nissenbaum MA, Raptopoulos V, Edelman RR. Abdominal diffusion mapping with use of a whole-body echo-planar system. Radiology. 1994; 190(2):475–478. http://dx.doi.org/10.1148/radiology.190.2.8284402. [PubMed: 8284402]
32. Luciani A, Vignaud A, Cavet M, Nhieu JT, Mallat A, Ruel L, et al. Liver cirrhosis: intravoxel incoherent motion MR imaging–pilot study. Radiology. 2008; 249(3):891–899. http://dx.doi.org/10.1148/radiol.2493080080. [PubMed: 19011186]

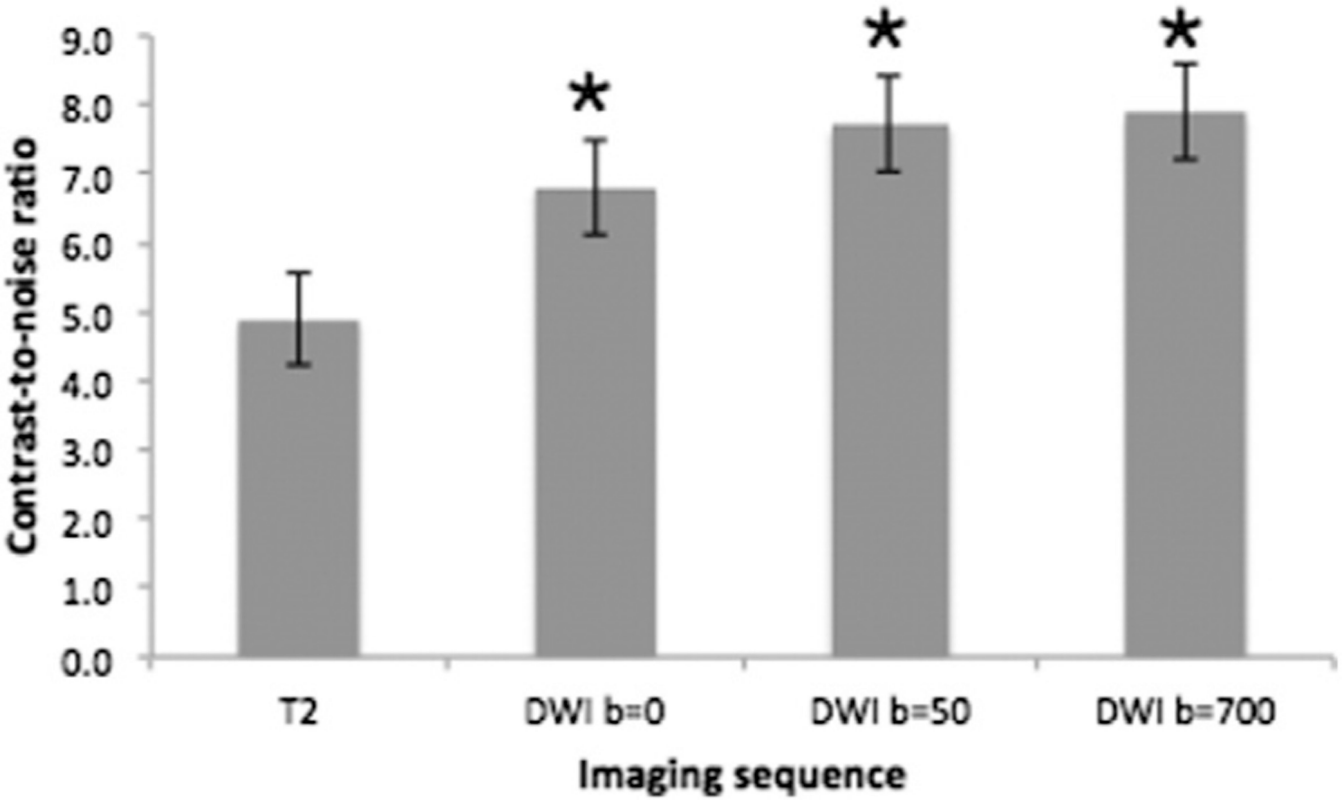

Fig. 1.

Lesion-to-liver contrast-to-noise ratios (CNRs) among T2-weighted and diffusion--weighted images for 49 identified LI-RADS 3–5 lesions demonstrating that diffusion weighted imaging (DWI) has higher CNR compared to single shot T2-weighted imaging (* $p < 0.0001$ for $b = 0$, $b = 50$ and $b = 700$) with error bars representing standard error of the mean.

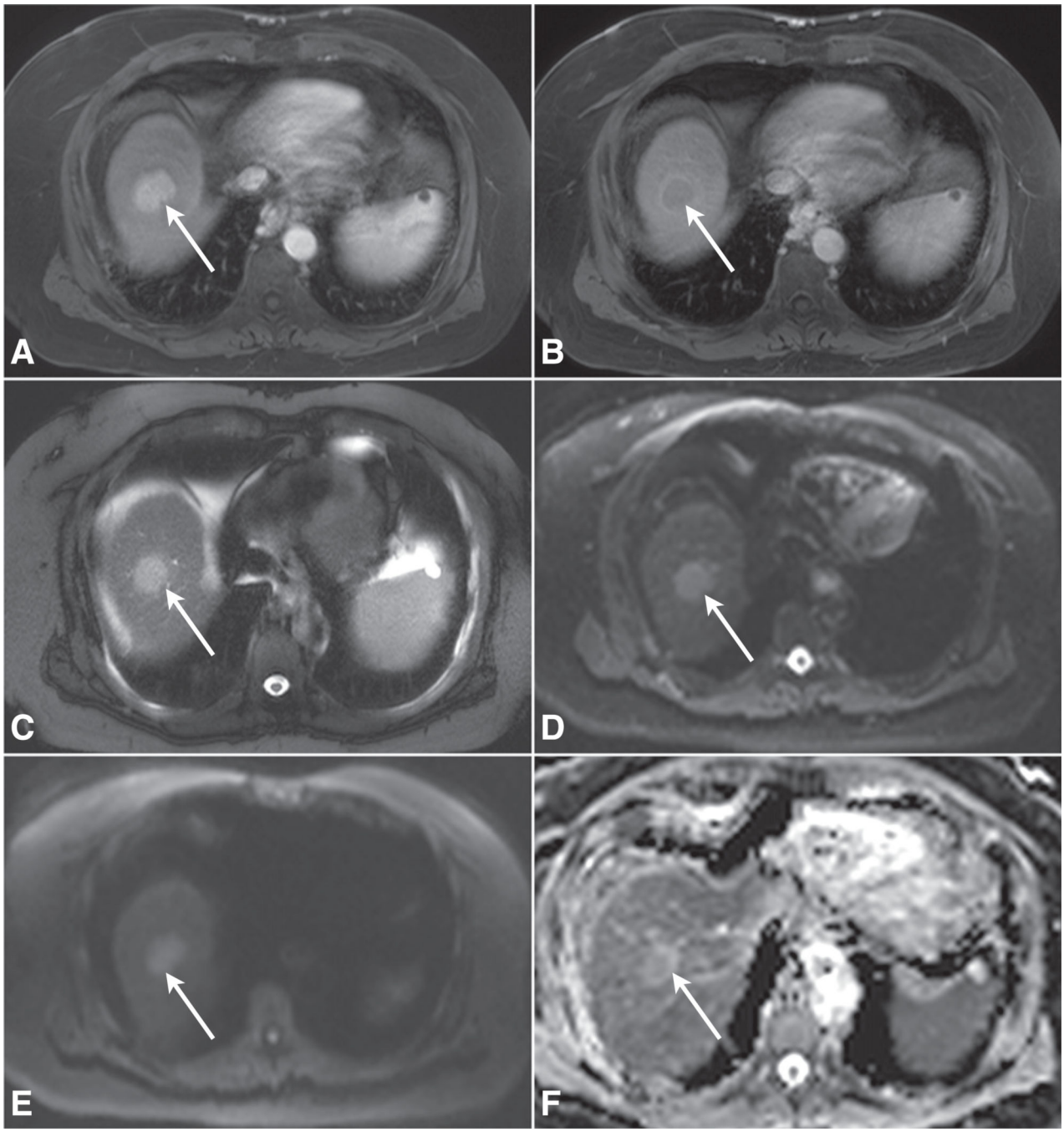

Fig. 2.

68-year-old male with a solitary arterially enhancing 3.0 cm hepatocellular carcinoma in segment VIII (A, arrow). 5-min delayed phase image (B, arrow) demonstrates washout appearance with associated capsule appearance, confirming LI-RADS 5 classification. The corresponding lesion was also seen on (C, arrow) T2 SSFSE images and on all DWI (b = 0 and 700 shown, D–E, arrows) with corresponding ADC map (F, arrow).

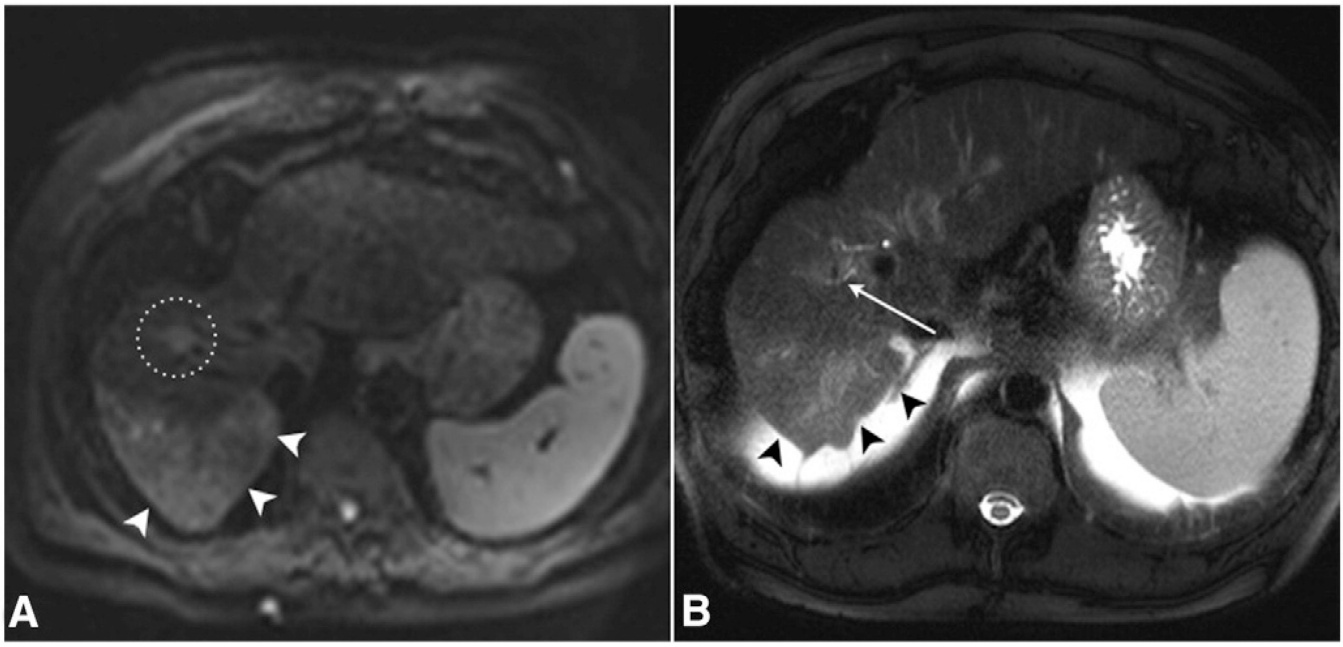

Fig. 3.

68-year-old male with acute transaminitis and a prior history of hepatocellular carcinoma tumor ablation. (A) DWI b = 50 image shows a 1.3 cm segment V lesion (dotted circle) corresponding to a LI-RADS 4 lesion on contrast-enhanced imaging. (B) T2-weighted SSFSE images are masked by signal from adjacent hepatic vasculature (white arrow). Note the crescent-shaped area of heterogeneous hyper-intensity in (A, white arrowheads) and (B, black arrowheads) corresponding to transient hepatic intensity difference on arterial phase images.

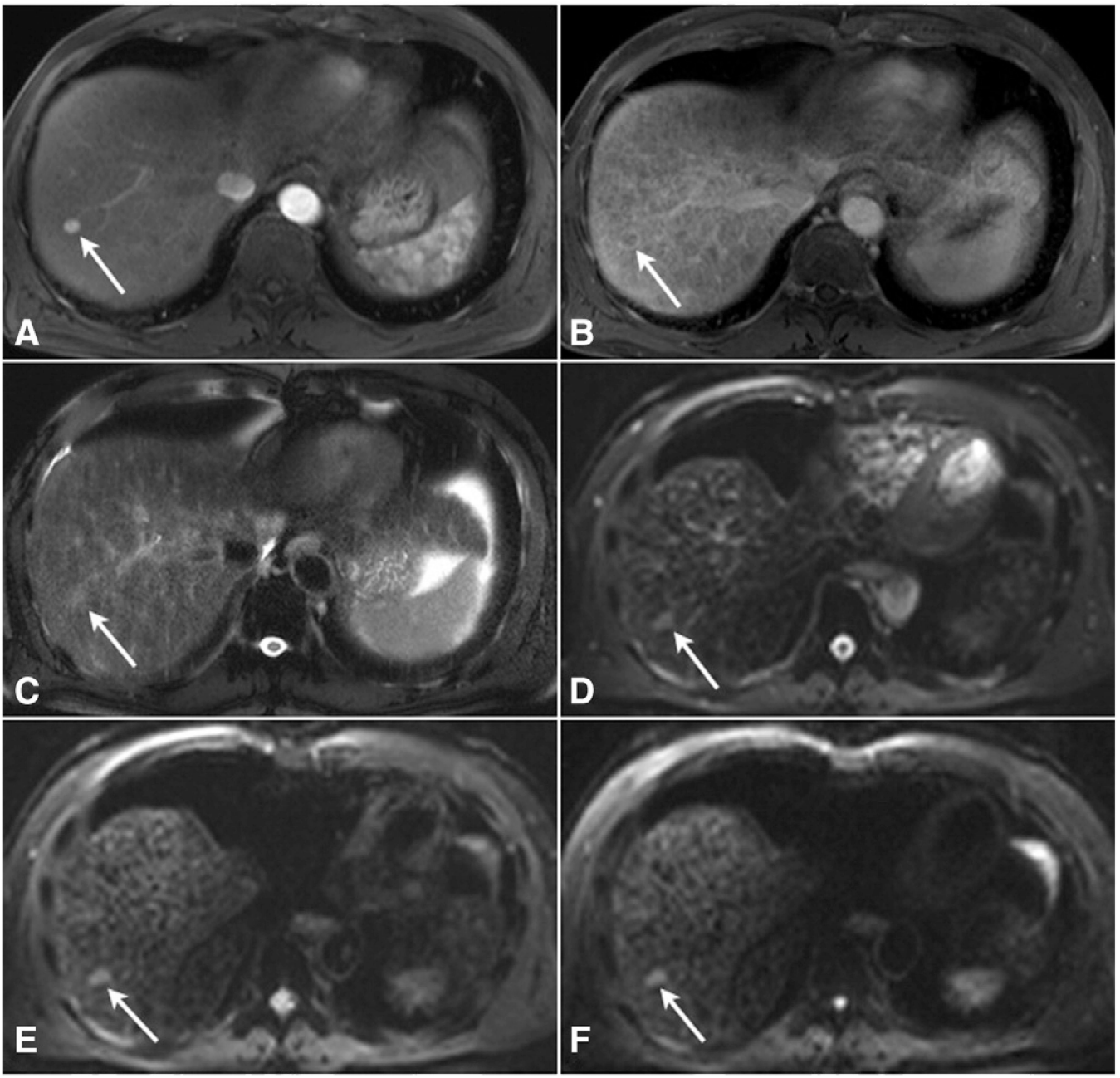

Fig. 4.

60-year-old male with cirrhosis due to Hepatitis C Virus. (A) A 1.1 cm arterially hyper-enhancing lesion is seen in segment VII (white arrow) with washout appearance and capsule appearance on 5-min delayed phase images (B). The corresponding lesion was identified by both readers on T2-weighted SSFSE (C) and DWI b = 0, 50, and 700 (D–F, respectively), although the higher CNR can be appreciated on DWI.

Table 1

Detection rates of T2-weighted imaging and diffusion-weighted imaging (DWI) with b-values of 0, 50, and 700.

Parameter	LI-RADS 3–5 lesions (n = 68)
T2w imaging	
Reader 1	0.56 (38/68)
Reader 2	0.63 (43/68)[b]
Consensus	0.59 (40/68)
DWI b = 0	
Reader 1	0.49 (33/68)
Reader 2	0.49 (33/68)
Consensus	0.53 (36/68)
DWI b = 50	
Reader 1	0.50 (34/68)
Reader 2	0.65 (44/68)[c]
Consensus	0.57 (39/68)
DWI b = 700	
Reader 1	0.62 (42/68)[a]
Reader 2	0.71 (48/68)[c]
Consensus	0.63 (43/68)[d]

DWI with a b-value of 700 had the highest detection rates compared to a b-value of 0.

[a] $p = 0.002$ between b = 0 and b = 700, and $p = 0.021$ between b = 50 and b = 700.

[b] $p = 0.031$ between T2 and b = 0.

[c] $p < 0.001$ between b = 0 and b = 50, and between b = 0 and b = 700.

[d] $p = 0.039$ between b = 0 and b = 700.

Table 2

Contrast-to-noise ratios (CNRs) of 49 lesions identified on T2-weighted images and/or diffusion weighted imaging (DWI) demonstrating higher CNR using DWI compared to single shot T2 imaging.

	Mean lesion-to-liver CNR			
	T2w imaging	**DWI b = 0**	**DWI b = 50**	**DWI b = 700**
HCC (n = 49)	4.64 ± 3.11	6.65 ± 5.01[a]	6.97 ± 5.27[a]	7.37 ± 5.96[a]
LI-RADS 5 (n = 18)	5.63 ± 3.31	9.01 ± 6.04	8.93 ± 6.78	9.83 ± 8.29
LI-RADS 4 (n = 27)	3.79 ± 2.86	5.62 ± 3.82	6.24 ± 3.85	6.23 ± 3.56
LI-RADS 3 (n = 4)	5.97 ± 2.72	2.95 ± 2.64	3.11 ± 2.65	3.96 ± 2.56

[a] $p < 0.001$ between all DWI sequences compared to T2w imaging.

Table 3

Apparent diffusion coefficient (ADC) values in mm^2/s of 49 lesions identified on T2-weighted images and/or diffusion weighted imaging (DWI).

	Lesion ADC (0–700) ± SD	Liver ADC (0–700) ± SD
HCC (n = 49 lesions)	1.22 ± 0.30	1.22 ± 0.21
LI-RADS 5 (n = 18)	1.21 ± 0.41	1.18 ± 0.25
LI-RADS 4 (n = 27)	1.21 ± 0.21	1.21 ± 0.19
LI-RADS 3 (n = 4)	1.35 ± 0.38	1.29 ± 0.19
Lesion size		
≥2 cm (n = 19)	1.09 ± 0.33[a]	1.22 ± 0.25
<2 cm (n = 30)	1.31 ± 0.26[b]	1.20 ± 0.19[b]

[a] p = 0.02 between lesions <2 cm and ≥2 cm in size.

[b] p = 0.045 between lesion ADC and liver ADC in lesions <2 cm in size.